metals

MDPI

Article

Investigation on Contact Heating of Aluminum Alloy Sheets in Hot Stamping Process

Huicheng Geng, Yilin Wang, Zijian Wang * and Yisheng Zhang

State Key Lab of Materials Processing and Die and Mould Technology, Huazhong University of Science and Technology, Wuhan 430074, China; ghc@hust.edu.cn (H.G.); wangyilin@hust.edu.cn (Y.W.); zhangys@mail.hust.edu.cn (Y.Z.)

* Correspondence: wangzijian@hust.edu.cn; Tel.: +86-027-8754-4457

Received: 26 October 2019; Accepted: 10 December 2019; Published: 12 December 2019

Abstract: Application of the hot stamping process on heat-treatable aluminum alloys effectively solves the problems of large springback and poor ductility during forming at room temperature, which expands the range of applications of aluminum alloys in the transportation industry. Sheet heating plays an important role in the hot stamping process, and increasing the heating rate can improve the hot stamping efficiency to some extent. In this paper, the feasibility of applying contact heating techniques with higher heating rates in the hot stamping process was studied. A contact heating device was designed, and the temperature distribution of the device contact surface was observed. Furthermore, the heating characteristics of 7075 aluminum alloy sheets during the contact heating process were explored by experiments and finite element simulation. Finally, the rapid solution treatment of aluminum alloy was carried out with a contact heating device, which was compared with the furnace heating solution treatment. The experimental and simulation results indicate that the device contact surface has a relatively uniform temperature distribution, and the aluminum alloy sheets can be heated to close to the set temperature in 15 s using contact heating techniques. Meanwhile, the rapid solution treatment of aluminum alloy sheets can be achieved within 15–20 s by contact heating techniques, obtaining superior mechanical properties. This suggests that the contact heating process can be used for rapid heating and rapid solution treatment of aluminum alloy sheets in hot stamping process.

Keywords: contact heating; aluminum alloys; hot stamping; rapid solution treatment; modeling

1. Introduction

The outstanding comprehensive properties of aluminum alloys make it a promising material in promoting lightweighting of automobiles [1–4]. However, high-strength aluminum alloys have poor ductility at room temperature, and in the traditional cold stamping process, aluminum alloys are prone to problems such as springback, cracking, and high forming resistance [5–8]. Thus, the application of high-strength aluminum alloys is limited. To improve the formability of aluminum alloy sheet and to reduce the springback after forming, a hot stamping process of heat-treatable aluminum alloys has been proposed, which has been extensively investigated and used for promoting automobile lightweighting [9–15].

Sheet heating is a necessary step in the hot stamping process and has an appreciable impact on the final performance of the parts. Radiation heating is currently the most commonly used sheet heating method in hot stamping processes. In this way, the aluminum alloy sheets have a uniform temperature distribution and the solute elements diffuse evenly in the matrix. However, due to the lower emissivity of aluminum alloy, the heating rate of aluminum alloy sheets by radiation heating is only about 0.4 °C/s [16], which seriously affects the hot stamping efficiency of the aluminum alloy. For

example, to achieve good performance, the heat treatment of 7075 aluminum alloy in hot stamping usually consists of solution treatment at 480 °C for 1 h and artificial aging at 120 °C for 24 h [17–19]. To shorten the heating time and improve the hot stamping productivity, attempts have been made to improve the process to achieve more efficient heat treatment of aluminum alloys [20,21]. Xu et al. [22] found that MgZn2 (η) particles could be completely dissolved after holding at 475 °C for only 5 min, whereas the complete dissolution of S-phase particles requires a stepped solution treatment. Jiang et al. [23] achieved the fast heat treatment of 7075 aluminum alloy by loading specimens at 500 °C, solutionizing in 470 °C/5 min + 485 °C/9 min and aging in 140 °C/6 h + 150 °C/1 h.

On the other hand, using sheet heating methods with high efficiency can also improve hot stamping productivity, such as resistance heating, induction heating, contact heating and direct flame impingement (DFI) heating. Studies show that quick heating will not deteriorate the performance of aluminum alloys [5,16,24]. Furthermore, a higher heating rate inhibits grain growth, which is beneficial for part performance.

Resistance heating is suitable for long and narrow sheets due to the heating method of electrical current conduction, and the metal sheets can be heated to the quenching temperature within 2 or 3 s [25]. To extend the application of the heating method, Mori et al. obtained circular heating zone for shearing by local resistance heating with a pair of electrode pins, but the heating setting is complicated [26,27]. Kolleck et al. [28] conducted investigations on induction heating, in which a two-step induction heating device was used, and the shortest heating time guaranteeing austenitization of 22MnB5 with a thickness of 1.5 mm was 35 s. However, it is also difficult to heat complex-shaped sheets using this method. The direct flame impingement heating method was proposed to heat high-strength aluminum alloys by hot gas or flame generated via combustion of fuel, and a heating rate of over 10 °C/s was obtained by DFI on AA6082 sheets of 1.5 mm [29]. The surface layer of DFI-heated samples is comparable to those heated by a conventional furnace, while the temperature uniformity of sheets heated by DFI may be poor.

The contact heating technique is a sheet heating method proposed in recent years in which the sheet is heated rapidly by contacting with the high-temperature contact plates [30]. Unlike the other rapid heating methods described above, the contact heating method can be used to heat complex-shaped sheets. Due to the large heat flux between the contact plates and the sheet during the heat conduction process, a higher heating rate is achieved. The existing research on the contact heating technique mainly focuses on heating high-strength steel sheets, and there are few studies on the contact heating process of aluminum alloys. Ploshikhin et al. [30] first conducted research on the contact heating technique in which a contact heating device was designed for the heating and tempering of steel blanks. Higher heating rates and temperatures reduce the cycle time for preheating of metal sheets to 20–40 s with contact heating. The University of Waterloo [31–33] also conducted a study on the contact heating process of high strength steel blanks, and successfully brought the monolith to its operating temperature of 1050 °C for one hour with SiC elements heating the monolith. In addition, the steel blanks were heated to Ac3 temperature within 60 s. It was found that the blank coating adhered to the monolith in the test. Therefore, the effects of different surface treatments on the adhesion of coating during contact heating process were studied. In addition, the tailored heating process of high-strength steel blanks with tailored contact surface was also carried out. In our previous study, the feasibility of continuous heating of aluminum alloy sheets by contact heating process was investigated and this study is an extension the previous study [34]. Zhang et al. [16] used the contact heating method to heat the 7075 aluminum alloy and compared the effects of contact heating solid solution treatment and traditional furnace solid solution treatment. It was indicated that the fine precipitated phase obtained by the contact heating process could make the material strength slightly higher than that of T6. Furthermore, during hot stamping, the lubricant is usually only painted on the regions of the die where severe deformation occurs, such as small corners, deep drawing areas, and so on. Painting the lubricant on each blank will cause a larger increase in cost, and requires a special lubricant painting device to realize automatic working. In addition, painting the lubricant on the Al alloy blanks directly

greatly affects the surface quality of the hot stamped Al alloys parts. Based on the above considerations, the lubricant was not considered in this studied contact heating stage.

The contact heating method is characterized by a higher heating rate and is suitable for sheets of different shapes, thus facilitating industrial application in the hot stamping process of aluminum alloys. However, the effects of heating temperature and holding time in the rapid heating process on the dissolution of the second phase is unclear. It is necessary to study the influence of the rapid heating process (the heating temperature and holding time) on the performance of aluminum alloy, and obtain the best heating conditions for the rapid solution treatment of aluminum alloys. In this paper, a contact heating device was designed and manufactured, and the research on the contact heating process of aluminum alloy sheets was carried out. The heating characteristics of aluminum alloy sheets during contact heating were also analyzed on the basis of experiments and simulation. Additionally, the research on the rapid solution treatment of aluminum alloys by contact heating method was conducted.

2. Experimental Device, Method, and Simulation

2.1. Contact Heating Device

Contact heating has more advantages than conventional furnace heating. However, due to the high-temperature accuracy of aluminum alloy sheets during hot stamping, there are some requirements for the design of contact heating devices: an excellent temperature uniformity of contact surface; a higher heating rate; and a lower temperature overshoot. Based on these factors, a contact heating experimental device was designed, the structural model of which is shown in Figure 1a. In the design stage, to achieve a device with better insulation performance and uniform contact surface temperature distribution, it was determined that the heating device should mainly consist of an upper and a lower contact plate, surrounding insulation asbestos and bottom insulation boards. The device was heated by the inner heating rods. The surrounding and bottom insulation material with low thermal conductivity could reduce the heat dissipation, while the temperature gradient of the contact surface could then be decreased, making the surface temperature uniform. The contact surface temperature uniformity of the contact heating device has considerable influence on the temperature uniformity of the heated sheet. Greater high-temperature thermal conductivity of the contact plates can effectively improve the contact surface temperature uniformity.

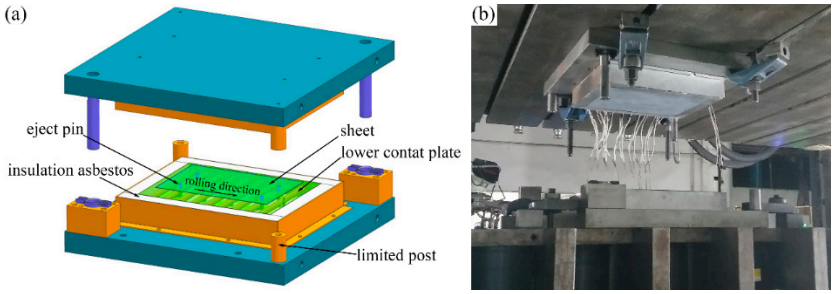

Figure 1. (**a**) The structural model and (**b**) the actual diagram of the contact heating device.

Since the heating temperature of the contact heating device is high, it was necessary for the material of the contact plates to possess high oxidation resistance and be able to be repeatedly heated to higher temperatures without a significant decrease in performance. Furthermore, the contact plate material should feature higher high-temperature compressive strength to resist the force between the sheet and the contact plates during the heating process. Finally, a hot work die steel called QRO 90 Supreme was selected because the excellent high-temperature strength, red hardness, and fatigue properties of the steel were able to meet the performance requirements of the contact plates. The thermo-physical parameters of QRO 90 Supreme die steel are shown in Table 1.

Table 1. Thermo-physical parameters of QRO 90 Supreme die steel.

Temperature (°C)	20	400	600
Density (kg/m^3)	7800	7700	7600
Elastic modulus (GPa)	210	180	145
Expansion coefficient (/°C)	-	12.6×10^{-6}	13.2×10^{-6}
Thermal conductivity (W/m·°C)	-	33	33

The heating device was equipped with some auxiliary systems: a heating system, a temperature controlling system and a temperature collecting system. The contact plates were heated by heating rods, and the rated power was 16 kW. K-type thermocouples were fixed inside the contact plates between each pair of heating rods for feedback adjustment of the device temperature. The eject pins were arranged in the lower contact plate to assist the placement and gripping of the sheets. The heating device was installed on a press, and the device was driven to open and close by the movement of the press slide, as shown in Figure 1b. The aluminum alloy sheet was placed on the lower contact plate, and the heating process is completed after the device is closed.

2.2. Experimental Method

A 7075 aluminum alloy sheet with a nominal thickness of 2 mm was chosen as the test material, which is a high-strength heat-treatable aluminum alloy. In addition, rectangular sheets (300 × 210 mm^2) were machined parallel to the rolling direction for experiments. The chemical composition of the aluminum alloy is given in Table 2. For the initial alloy tempering, the tensile strength was 558.7 MPa, the elongation was 13.4%, and the hardness was 173.9 HV.

Table 2. Chemical composition of 7075 aluminum alloy (wt.%).

Mg	Zn	Mn	Cu	Fe	Cr	Si	Al
3.161	5.895	0.1778	1.63	0.1309	0.2113	0.03	Bal.

The temperature distribution of the contact surface was observed through an infrared thermal imager (FLIR A320, FLIR Systems Inc., Wilsonville, OR, America), and the temperature uniformity of the contact surface was analyzed. The temperature collecting process of the contact surface was affected by the properties of the contact surface, and the observed results may be subject to large error. Therefore, necessary measures were taken to improve the temperature observation process.

As shown in Figure 2, there were holes at the edges of the sheet, and K-type thermocouples were fixed in the holes for temperature collection. The heating characteristics of the device were studied and compared with the heating of the furnace.

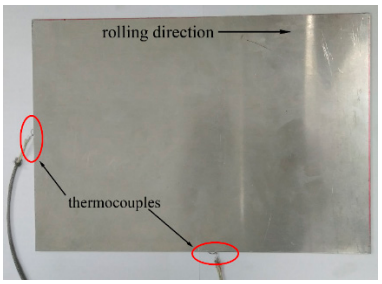

Figure 2. Macroscopical image of the specimen and the fixation of thermocouples.

The rapid solution treatment of 7075 aluminum alloy sheets was also carried out with the contact heating device, and the feasibility of the method was analyzed. As shown in Figure 3, the rapid solution test was subjected to a process comprising the following procedures: (a) contact heating and

holding at different temperatures and times (solution treatment); (b) water quenching the specimen to room temperature; (c) artificial aging at 120 °C for 24 h; and finally (d) cooling to room temperature. The solution temperatures of the sheets were 470 °C, 480 °C, 490 °C, and 500 °C, respectively. The solution times of the sheets were 15 s, 20 s, 30 s, 40 s, 50 s, and 60 s, respectively.

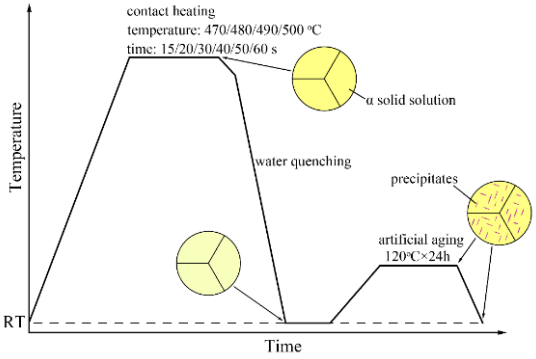

Figure 3. Schematic diagram of the experimental process of the rapid solution treatment.

2.3. Simulation

A finite element model of the contact heating device was established to analyze the contact heating process of aluminum alloy sheets, and the heating characteristics during the process were studied. The simulation model is shown in Figure 4, and the same structural parameters as the actual device were set on this model. To simplify the modeling process, the simulation model consists only of contact plates and surrounding insulation materials.

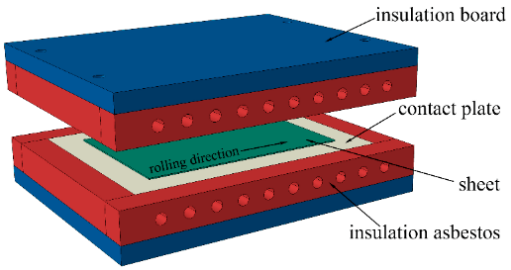

Figure 4. The structure of the simulation model.

In this simulation, the effects of radiation and convection conditions on the heating process were considered. The convective heat transfer between the device and ambient varies with the device temperature. Therefore, considering the large temperature range of the device, the convective heat transfer coefficient varies with temperature:

$$h = 2(T_w - T_f)^{1/3}, \tag{1}$$

where h is the convective heat transfer coefficient (W/(m^2·K)), T_w and T_f are the device surface temperature and the ambient temperature, respectively.

At the same time, the contact heating device also radiates heat to the ambient constantly, and the heat loss per unit area due to surface radiation can be expressed as:

$$q = \sigma\varepsilon\left[(T - T_Z)^4 - (T_0 - T_Z)^4\right], \tag{2}$$

where q refers to the radiative heat flux (W/m^2), σ is Stefan Boltzmann constant, and $\sigma = 5.67 \times 10^{-8}$ W/(m^2·K^4), ε is the surface emissivity, T, T_0, and T_Z are the device surface temperature, ambient temperature, and absolute zero temperature, respectively.

Both higher surface emissivity of the contact surface and the increase of the device temperature cause a large amount of heat loss. The emissivity of contact surface in the simulation is set as 0.8. Based on Equations (1) and (2), the heat dissipation per unit area caused by convection and radiation is shown in Figure 5.

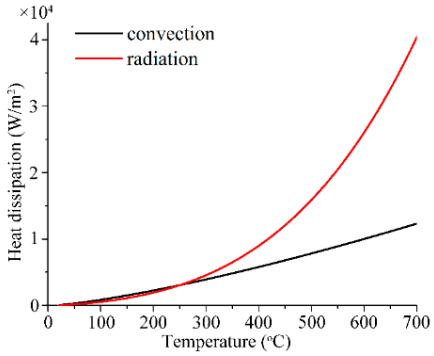

Figure 5. Comparison of heat dissipation caused by convection and radiation.

The simulation procedure is shown in Figure 6. The PID control algorithm was implanted into the simulation using a user-defined subroutine 'pid.for' to model temperature controlling during the heating process of the device. Combined with the history temperature output values of the selected nodes in the model, the surface heat flux on the inner wall of the heating holes was adjusted to achieve temperature control of the heating model. In addition, the temperature distribution of the device was obtained when the temperature was 480 °C. Then the simulated results of the device heating stage were transferred to the contact heating simulation of aluminum alloy sheet. The sheet heating time was 30 s, and the sheet dimension was the same as the specimen in the experiment, while its initial temperature was 20 °C. The interfacial heat transfer coefficient between the contact plate and the aluminum alloy sheet was considered as 800 W/(m^2·K) [35]. Finally, the temperature distribution of the sheet was obtained and studied as well as the heating curves of the sheet.

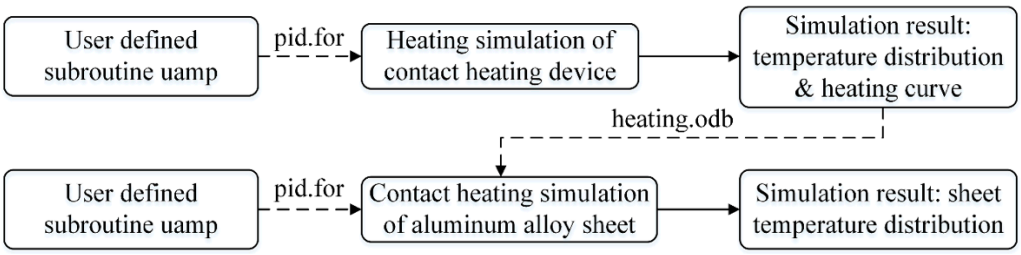

Figure 6. Visual presentation of the simulation procedure.

3. Results and Discussion

3.1. Simulation Results

3.1.1. Temperature Distribution of Simulation Model

The heating temperature was set to 480 °C, and the model was heated and held for 1 h. When the temperature of the device became stable, the temperature distribution of the model is shown in Figure 7a, wherein one quarter of the model is omitted to enable an inspection of the temperature distribution inside the device. The heating curves of the nodes in the model are shown in Figure 7b,c. Due to the superior insulation properties of the insulation materials, the contact plates possessed higher temperature, and the temperature difference of the contact surface was less than 10 °C, which was beneficial to the uniformity of sheet temperature distribution during the contact heating process.

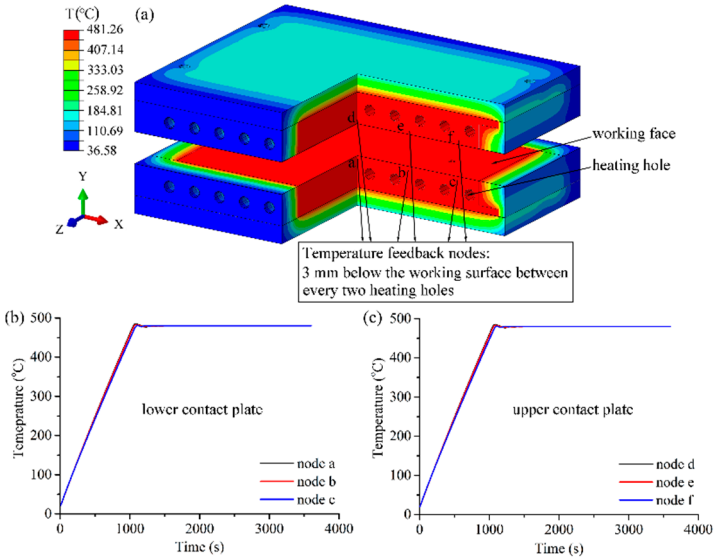

Figure 7. The simulation model is heated to 480 °C and held to stabilize the temperature: (**a**) temperature distribution of 3/4 simulation model; (**b**) heating curves of temperature feedback nodes in the lower contact plate; (**c**) heating curves of temperature feedback nodes in the upper contact plate.

3.1.2. Contact Heating Process of Aluminum Alloy Sheets

Based on the simulation results obtained from device heating stage, the simulation of contact heating process of the aluminum alloy sheet was performed. The temperature distribution of the lower contact plate before and after contact heating is shown in Figure 8a,b. The temperature distribution of the sheet after contact heating is shown in Figure 8c and the heating curve of the sheet is shown in Figure 8d. It can be seen from the simulation results that the rapid and uniform heating process of aluminum alloy sheet can be achieved by contact heating techniques. Furthermore, due to the uniform temperature distribution of the contact surface and the large thermal conductivity of aluminum alloy, the sheet temperature difference after contact heating was smaller than 5 °C.

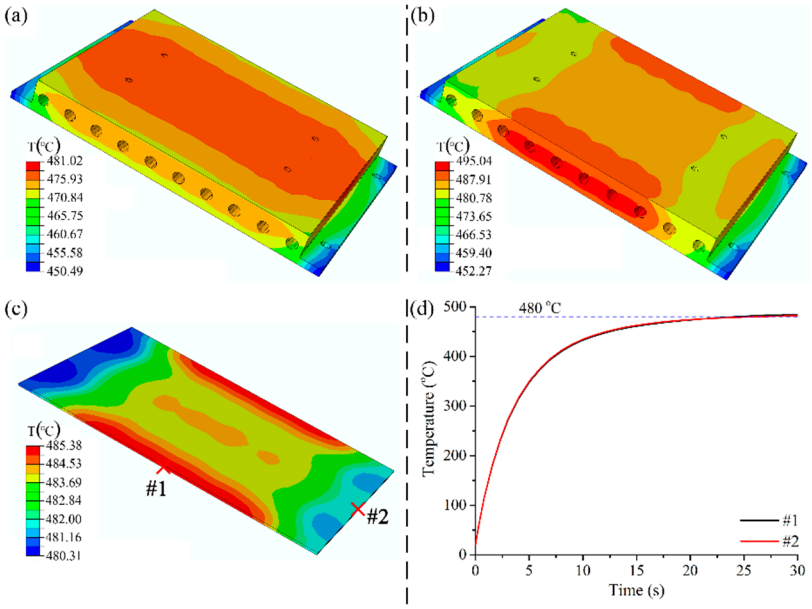

Figure 8. (**a**) Lower contact plate temperature distribution before contact heating process. (**b**) Lower contact plate temperature distribution after contact heating process. (**c**) Temperature distribution of the sheet after contact heating process. (**d**) Heating curves of nodes in the sheet.

3.2. Experimental Results

3.2.1. Analysis of Contact Surface Temperature Distribution

During the observation of the contact surface temperature, to improve the observation accuracy of the infrared thermal imager, four digital thermometers were applied to calibrate the parameters of the infrared thermal imager software through their display. Meanwhile, the contact surface was sprayed with high-temperature-resistance paint (with a stable emissivity of 0.95–0.98) to improve the contact surface emissivity. Figure 9 shows the countermeasures to improve the observation accuracy.

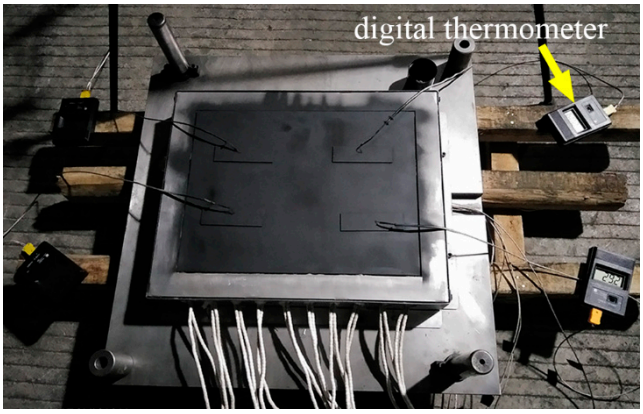

Figure 9. The countermeasures to improve the observation accuracy of the infrared thermal imager.

After the calibration, the digital thermometers were removed. The temperature distribution of the upper contact surface when the heating temperature was set to 500 °C is shown in Figure 10a. Five lines are equally spaced on the contact surface for temperature analysis, and the temperature distribution along these five lines is shown in Figure 10b. The observed temperature distribution results showed that the temperature along these lines was lower at the end region, and turned relatively uniform in the middle region, while the temperature difference in the central region is less than 20 °C. In addition, the temperature uniformity of the surface can be improved by an extended holding process.

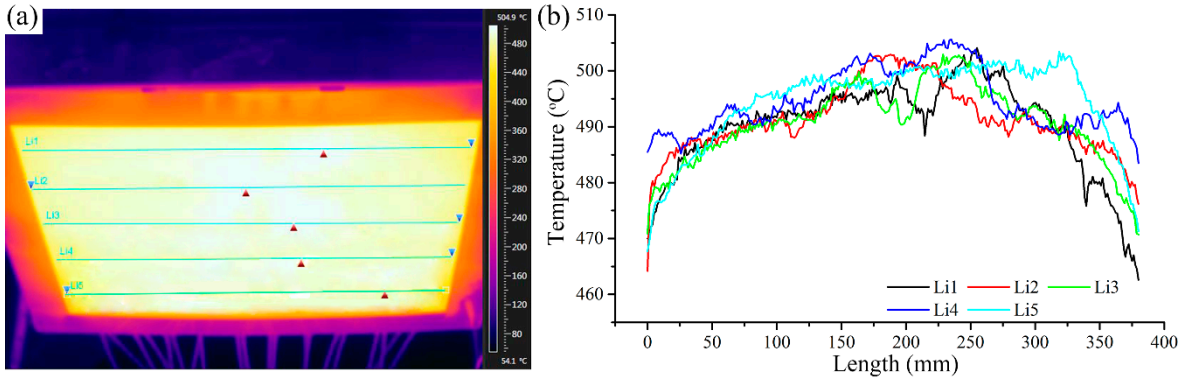

Figure 10. (**a**) Temperature distribution of the upper contact surface when the heating temperature is 500 °C. (**b**) Temperature distribution along five lines equally spaced in the contact surface.

To study the relationship between the actual temperature of the contact surface and the set temperature, the surface center temperature T was taken by infrared thermal imager, and the relationship between surface center temperature T and set temperature t were fitted. A correlational formula was developed for the relationship: $T(°C) = 0.964t + 5.689$, as shown in Figure 11. The surface temperature will be affected by the ambient, so the experimental environment should be kept free of wind.

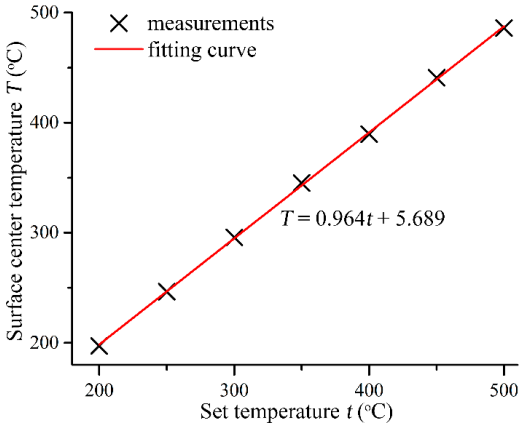

Figure 11. Relationship between surface center temperature T and set temperature t.

3.2.2. Heating Curves of Aluminum Alloy Sheets during Contact Heating

The contact heating of aluminum alloy sheets was performed, and the device temperature was set to 200 °C, 300 °C, 400 °C, and 500 °C, respectively. The heating curves of the sheets at different heating temperatures are shown in Figure 12. It can be seen that during the contact heating process, the sheet temperature rose rapidly and soon approached the set temperature at the beginning of the heating process. When the sheet temperature was close to the set temperature, the heating rate decreased. When the sheet temperature reached the set temperature, the overheating effects could be ignored.

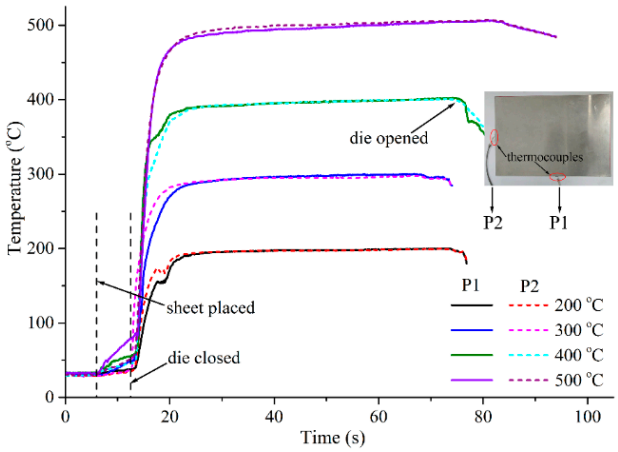

Figure 12. Heating curves of aluminum alloy sheets during contact heating at different heating temperatures.

To evaluate the heating rate of the sheet during contact heating process, when the device was set to a different heating temperature T_S, the time for the sheet to heat up to (T_S−20) °C and (T_S−10) °C from the device closing was summarized, as shown in Figure 13. The results showed that as the heating temperature increased, the time required for the sheets to heat up increased slightly, although not significantly. When the set temperature was high, the temperature difference between the contact plates and the sheet is large, which resulted in a larger heat flux between them. Hence, the sheet heating rate became larger and the heating time did not increase significantly at a higher heating temperature. Meanwhile, it was revealed that when different heating temperatures were set, the sheets could be heated to close to the set temperature within 15 s (the difference between the sheet temperature and the set temperature was less than 10 °C).

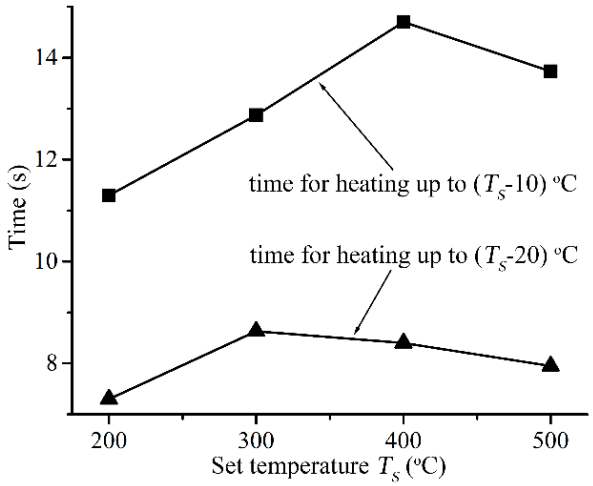

Figure 13. Time for the sheet to heat up to (T_S-20) °C and (T_S-10) °C from device closing.

3.2.3. Rapid Solution Treatment of 7075 Aluminum Alloy Sheet

Figure 14 shows the tensile strength, elongation and hardness of 7075 aluminum alloy after rapid solution treatment with different solution temperatures and times by contact heating and 120 °C/24 h artificial aging. Figure 14a shows that by contact heating techniques, when the solution temperature and the solution time were 470–500 °C and 15–60 s respectively, the tensile strength of the specimens exceeded that of the initial alloy temper. Even if the solution time was as short as 15 s, the specimens could still achieve higher strength, and the extension of solution time did not result in a significant increase in tensile strength. During contact heating, the sheet temperature quickly approached the solution temperature (the set temperature), which caused the second phase in the matrix to dissolve rapidly in a short time. In addition, the specimen reached the maximum tensile strength of 580.1 MPa with a solution temperature of 470 °C and a solution time of 40 s.

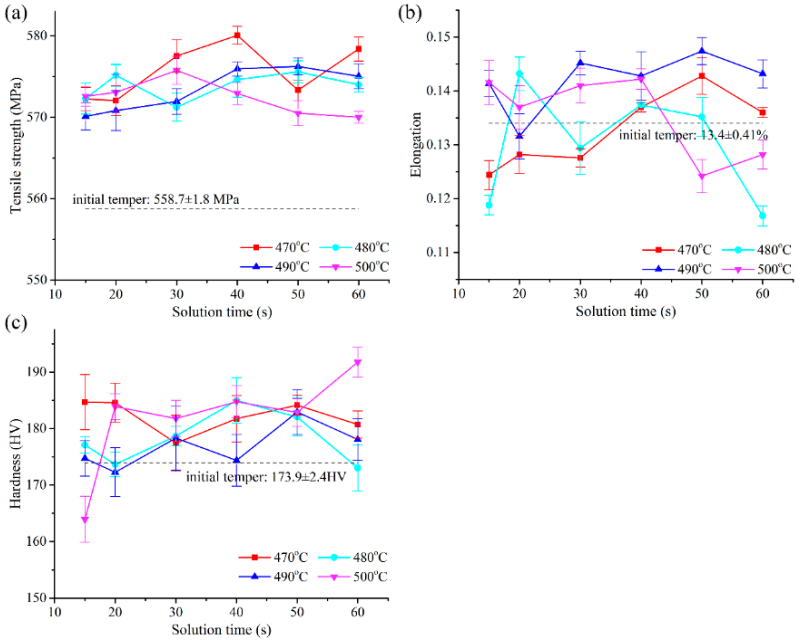

Figure 14. Mechanical properties of 7075 aluminum alloy after rapid solution treatment with different solution temperatures and times by contact heating process and artificial aging: (**a**) tensile strength; (**b**) elongation; (**c**) hardness.

Figure 14b shows that the elongation of the specimens after rapid solution treatment with different solution conditions and artificial aging ranged from 11 to 15%, which was close to the elongation of the initial temper (13.4%). With increasing solution temperature, the elongation of the specimens exhibited a certain increase. In addition, the specimen showed larger elongation when the solution temperature was 490 °C. However, there was a slight drop in elongation at 500 °C. At the same time, there was no clear tendency of the effects of solution time on elongation.

Figure 14c shows the hardness of the specimens after contact heating solution treatment, and artificial aging was generally higher than that of the initial temper. However, lower hardness than the initial temper was obtained in the specimens when contact heating was set at 500 °C for 15 s, and the specimens featured their highest hardness (191.8 ± 2.6 HV) when heated at 500 °C for 60 s.

Therefore, using contact heating techniques, the rapid solution treatment of 7075 aluminum alloy sheets can be achieved. Considering the efficiency of solution treatment in production and avoiding overheating of aluminum alloy, the appropriate solution temperature and time were 470–480 °C and 15–20 s, respectively. In addition, better mechanical properties can be obtained under these conditions.

Figure 15 shows the metallography of 7075 aluminum alloy solutionized at different temperatures for 30 s by contact heating with artificial aging not performed. It is depicted that after solution treatment by the contact heating device, some small second-phase particles existing in the initial temper were dissolved, and there were precipitates with higher melting points remaining in the matrix. The insufficient dissolution of the second phase may be due to the short solution time. Meanwhile, overheating was not observed in the microstructure throughout the entire solution temperature range, which may also be related to the shorter solution time. As the solution temperature increased, the amount of undissolved particles in the matrix decreased. Higher solution temperature contributed to the dissolution of the second phase, while allowing the solutes in the matrix to diffuse faster. However, in Figure 15d, it was found that although the amount of second phase decreased, the dimensions of the particles increased significantly when the solution temperature was 500 °C.

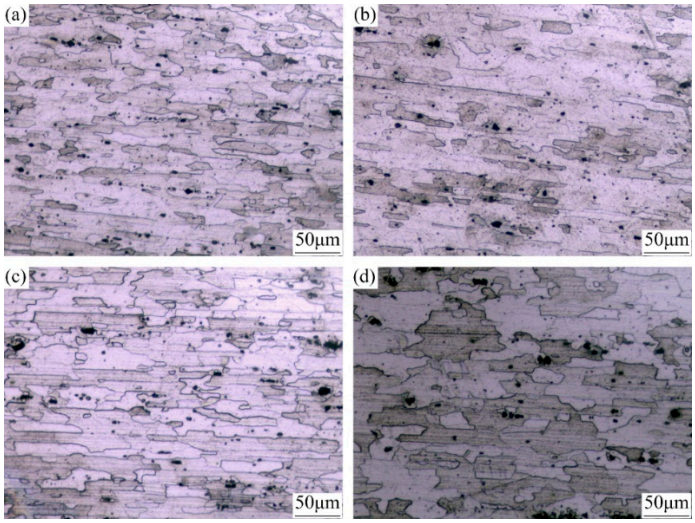

Figure 15. Metallography of 7075 aluminum alloy treated with different solution temperatures for 30 s: (**a**) 470 °C; (**b**) 480 °C; (**c**) 490 °C; (**d**) 500 °C.

The contact heating and conventional furnace heating methods were studied, and the effects of the two heating methods on the heating rate and performance of aluminum alloy sheets were compared. When the heating temperature was 480 °C, the heating curves of 7075 aluminum alloy with the two heating methods were recorded by thermocouples, as described in Figure 16a. It can be seen that the heating rate by contact heating method was about 28.7 °C /s, which was much higher than that of the furnace heating. Figure 16b shows that specimens with solution treatment by contact heating can obtain higher tensile strength than that by furnace heating, but the elongation was small. Figure 17 shows

that after solutionization by contact heating and furnace heating, plenty of the precipitates dissolved in the matrix. Meanwhile, during furnace heating, the precipitates dissolved more completely due to the longer heating time, there was less residual precipitates in the matrix, and the solutes were able to diffuse more evenly. Therefore, the specimens solutionized by furnace heating have a larger elongation.

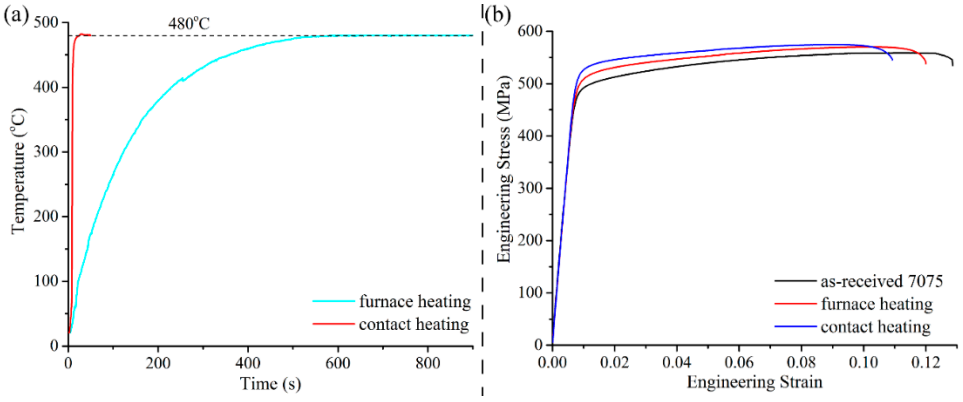

Figure 16. (**a**) Heating curves of 7075 aluminum alloy sheets during contact heating and furnace heating. (**b**) The tensile stress characteristics of 7075 aluminum alloy under different conditions: as-received 7075; contact heating solution treatment and furnace heating solution treatment followed by artificial aging.

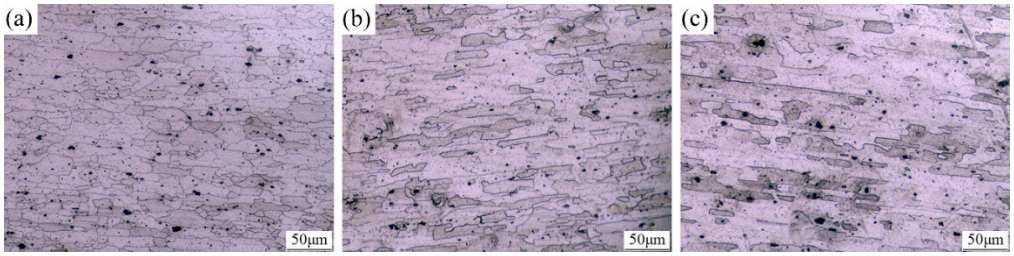

Figure 17. Metallography of 7075 aluminum alloy in different conditions: (**a**) original structure; (**b**) solutionizing at 480 °C for 15 min by furnace heating and quenched by water; (**c**) solutionizing at 480 °C for 30 s by contact heating and quenched by water.

4. Conclusions

In this paper, the contact heating method was applied for the rapid heating process of 7075 aluminum alloy, and the device temperature distribution and heating characteristics during contact heating were studied by experiments and finite element simulation. The feasibility of rapid solution treatment of 7075 aluminum alloy sheets by contact heating method was explored and the effects of contact heating and furnace heating were compared. The main conclusions in this paper can be summarized as follows:

(1) The contact heating device suitable for aluminum alloy sheets had a relatively uniform contact surface temperature distribution, and the temperature difference in the middle portion of the surface was less than 20 °C.

(2) Rapid heating of aluminum alloy sheets can be achieved by contact heating techniques. The time needed for sheet heating had little relationship with the set temperature, and the 7075 aluminum alloy sheets with the thickness of 2 mm can be heated near the set temperature within 15 s.

(3) Rapid solution treatment experiments of 7075 aluminum alloy were conducted using a contact heating device. It was found that the optimum solution temperature was 470–480 °C and the solution time was shortened to 15–20 s by contact heating techniques. Results showed that the maximum tensile strength under the optimum conditions reached 575.2 MPa after artificial aging, which was higher than that of the initial temper, and the elongation was close to that of the initial temper.

(4) The sheets with contact heating solution treatment possessed a greater tensile strength and a lower elongation than those of the furnace heating solution treatment, which was related to the dissolution of the precipitates during the heating process.

Author Contributions: Conceptualization, Y.Z.; methodology, Z.W. and Y.W.; validation, H.G. and Z.W.; investigation, H.G. and Z.W.; resources, Y.Z.

Funding: This research was funded by the National Natural Science Foundation of China (Grant No. U1760205 and U1564203) and the National Major Science Technology Project of China (Grant No. 2018zx04023001).

Acknowledgments: The authors would like to acknowledge the State Key Lab of Materials Processing and Die and Mould Technology for their assistance in the tensile experiments.

Conflicts of Interest: The authors declare no conflict of interest.

References

1. Zheng, K.; Politis, D.J.; Wang, L.; Lin, J. A review on forming techniques for manufacturing lightweight complex-shaped aluminium panel components. *Int. J. Lightweight Mater. Manuf.* **2018**, *1*, 55–80. [CrossRef]
2. Han, N.M.; Zhang, X.M.; Liu, S.D.; He, D.G.; Zhang, R. Effect of solution treatment on the strength and fracture toughness of aluminum alloy 7050. *J. Alloys Compd.* **2011**, *509*, 4138–4145. [CrossRef]
3. Zhang, Y.; Jin, W.; Hao, X.; Qiu, F.; Zhao, Q. Improving elevated-temperature strength of an Al-Mn-Si alloy by strain-induced precipitation. *Metals* **2018**, *8*, 446. [CrossRef]
4. Zhang, P.; Yan, H.; Liu, W.; Zou, X.; Tang, B. Effect of T6 heat treatment on microstructure and hardness of nanosized Al_2O_3 reinforced 7075 aluminum matrix composites. *Metals* **2019**, *9*, 44. [CrossRef]
5. Maeno, T.; Mori, K.; Yachi, R. Hot stamping of high-strength aluminium alloy aircraft parts using quick heating. *CIRP Ann.* **2017**, *66*, 269–272. [CrossRef]
6. Liu, Y.; Zhu, Z.; Wang, Z.; Zhu, B.; Wang, Y.; Zhang, Y. Flow and friction behaviors of 6061 aluminum alloy at elevated temperatures and hot stamping of a B-pillar. *Int. J. Adv. Manuf. Technol.* **2018**, *96*, 4063–4083. [CrossRef]
7. Liu, Y.; Zhu, Z.; Wang, Z.; Zhu, B.; Wang, Y.; Zhang, Y. Formability and lubrication of a B-pillar in hot stamping with 6061 and 7075 aluminum alloy sheets. *Procedia Eng.* **2017**, *207*, 723–728. [CrossRef]
8. Sun, L.; Cai, Z.; He, D.; Li, L. Aluminum alloy sheet-forming limit curve prediction based on original measured stress–strain data and its application in stretch-forming process. *Metals* **2019**, *9*, 1129. [CrossRef]
9. Garrett, R.P.; Lin, J.; Dean, T.A. An investigation of the effects of solution heat treatment on mechanical properties for AA 6xxx alloys: Experimentation and modelling. *Int. J. Plast.* **2005**, *21*, 1640–1657. [CrossRef]
10. Zheng, K.; Dong, Y.; Zheng, D.; Lin, J.; Dean, T.A. An experimental investigation on the deformation and post-formed strength of heat-treatable aluminium alloys using different elevated temperature forming processes. *J. Mater. Process. Technol.* **2019**, *268*, 87–96. [CrossRef]
11. Harrison, N.R.; Luckey, S.G. Hot stamping of a B-pillar outer from high strength aluminum sheet AA7075. *SAE Int. J. Mate. Manuf.* **2014**, *7*, 567–573. [CrossRef]
12. Zhou, J.; Wang, B.; Lin, J.; Fu, L.; Ma, W. Forming defects in aluminum alloy hot stamping of side-door impact beam. *Trans. Nonferrous Met. Soc. China* **2014**, *24*, 3611–3620. [CrossRef]
13. Xiao, W.; Wang, B.; Zheng, K. An experimental and numerical investigation on the formability of AA7075 sheet in hot stamping condition. *Int. J. Adv. Manuf. Technol.* **2017**, *92*, 3299–3309. [CrossRef]
14. Liang, W.; Tao, W.; Zhu, B.; Zhang, Y. Influence of heating parameters on properties of the Al-Si coating applied to hot stamping. *Sci. China Technol. Sci.* **2017**, *60*, 1088–1102. [CrossRef]
15. Schuster, P.; Österreicher, J.; Kirov, G.; Sommitsch, C.; Kessler, O.; Mukeli, E. Characterisation and comparison of process chains for producing automotive structural parts from 7xxx aluminium sheets. *Metals* **2019**, *9*, 305. [CrossRef]
16. Zhang, Z.; Yu, J.; He, D. Influence of contact solid-solution treatment on microstructures and mechanical properties of 7075 aluminum alloy. *Mater. Sci. Eng. A* **2019**, *743*, 500–503. [CrossRef]
17. Rojas, J.I.; Crespo, D. Dynamic microstructural evolution of an Al-Zn-Mg-Cu alloy (7075) during continuous heating and the influence on the viscoelastic response. *Mater. Charact.* **2017**, *134*, 319–328. [CrossRef]
18. Zou, X.; Yan, H.; Chen, X. Evolution of second phases and mechanical properties of 7075 Al alloy processed by solution heat treatment. *Trans. Nonferrous Met. Soc. China* **2017**, *27*, 2146–2155. [CrossRef]

19. He, X.; Pan, Q.; Li, H.; Huang, Z.; Liu, S.; Li, K.; Li, X. Effect of artificial aging, delayed aging, and pre-aging on microstructure and properties of 6082 aluminum alloy. *Metals* **2019**, *9*, 173. [CrossRef]
20. Rometsch, P.A.; Zhang, Y.; Knight, S. Heat treatment of 7xxx series aluminium alloys-some recent developments. *Trans. Nonferrous Met. Soc. China* **2014**, *24*, 2003–2017. [CrossRef]
21. Marlaud, T.; Deschamps, A.; Bley, F.; Lefebvre, W.; Baroux, B. Evolution of precipitate microstructures during the retrogression and re-ageing heat treatment of an Al-Zn-Mg-Cu Alloy. *Acta Mater.* **2010**, *58*, 4814–4826. [CrossRef]
22. Xu, D.K.; Rometsch, P.A.; Birbilis, N. Improved solution treatment for an as-rolled Al-Zn-Mg-Cu alloy. Part II. Microstructure and mechanical properties. *Mater. Sci. Eng. A* **2012**, *534*, 244–252. [CrossRef]
23. Jiang, S.; Nin, A.; Xian, S. Investigation on fast solid solution treatment of high strength aluminum alloy. *J. Shaoyang Univ. (Nat. Sci.)* **2005**, *2*, 25–27.
24. Chang, Y.; Hung, F.; Lui, T. Enhancing the tensile yield strength of A6082 aluminum alloy with rapid heat solutionizing. *Mater. Sci. Eng. A* **2017**, *702*, 438–445. [CrossRef]
25. Mori, K.; Maeno, T.; Mongkolkaji, K. Tailored die quenching of steel parts having strength distribution using bypass resistance heating in hot stamping. *J. Mater. Process. Technol.* **2013**, *213*, 508–514. [CrossRef]
26. Mori, K.; Maeno, T.; Fuzisaka, S. Punching of ultra-high strength steel sheets using local resistance heating of shearing zone. *J. Mater. Process. Technol.* **2012**, *212*, 534–540. [CrossRef]
27. Mori, K.; Maeno, T.; Maruo, Y. Punching of small hole of die-quenched steel sheets using local resistance heating. *CIRP Ann.* **2012**, *61*, 255–258. [CrossRef]
28. Kolleck, R.; Veit, R.; Merklein, M.; Lechler, J.; Geiger, M. Investigation on induction heating for hot stamping of boron alloyed steels. *CIRP Ann.* **2009**, *58*, 275–278. [CrossRef]
29. Shao, Z.; Jiang, J.; Lin, J. Feasibility study on direct flame impingement heating applied for the solution heat treatment, forming and cold die quenching technique. *J. Manuf. Process.* **2018**, *36*, 398–404. [CrossRef]
30. Ploshikhin, V.; Prihodovsky, A.; Kaiser, J.; Bisping, R.; Lindner, H.; Lengsdorf, C.; Roll, K. New heating technology for the furnace-free press hardening process. In *Tools and Technologies for Processing Ultra-High Strength Materials*; Graz, Austria, 2011.
31. Rasera, J.N.; Daun, K.J.; Shi, C.J.; D'Souza, M. Direct contact heating for hot forming die quenching. *Appl. Therm. Eng.* **2016**, *98*, 1165–1173. [CrossRef]
32. Rasera, J. Development of a Novel Technology for Rapidly Austenitizing Usibor® 1500P Steel. Master's Thesis, University of Waterloo, Waterloo, ON, Canada, 2015.
33. Field, N. Austenitization of Ultra-High Strength Steel by Direct Contact Heating for Hot Forming Die Quenching. Master's Thesis, University of Waterloo, Waterloo, ON, Canada, 2017.
34. Geng, H.C.; Wang, Z.J.; Wang, K.; Wang, Y.L.; Zhang, Y.S. Simulation on direct contact heating of aluminum alloys. In Proceedings of the 4th International Conference on Advanced High Strength Steel and Press Hardening (ICHSU2018), Hefei, China, 20–22 August 2018; pp. 249–254.
35. Ji, K.; Fakir, O.E.; Gao, H.; Wang, L. Determination of heat transfer coefficient for hot stamping process. *Mater. Today Proc.* **2015**, *2*, S434–S439. [CrossRef]